PHYSICAL REVIEW B VOLUME 25, NUMBER 2 15 JANUARY 1982

Empirical band calculations of the optical properties of *d*-band metals. IV. Optical absorption, photoemission, and magneto-optical properties of ferromagnetic nickel

N. V. Smith, R. Lässer,* and S. Chiang†
Bell Laboratories, Murray Hill, New Jersey 07974
(Received 14 July 1981)

An empirically adjusted band structure for ferromagnetic Ni has been constructed using a combined interpolation scheme. The principal adjustments consist of narrowing the *d* band by ~25% and raising it upwards in energy relative to the *sp* manifold in order to reproduce recent angle-resolved photoemission data. The exchange splitting is chosen to reproduce the experimental magneton number. This yields an exchange splitting ($\Delta_{ex}=0.310$ eV) and a Stoner gap ($\delta=0.100$ eV) in excellent agreement with other photoemission data. The bands are then used to compute the optical absorption and magneto-optical response with full inclusion of momentum matrix elements. After inclusion of lifetime effects, the optical absorption is found to be in good agreement with experiment over the $\hbar\omega < 30$ eV photon energy range, permitting reliable identification of structures and their $\vec{k}$-space locations. The calculated magneto-optical response is in good agreement with experiment in the range $\hbar\omega < 6$ eV, but only for the energy location of structures. The empirical adjustments are compared with recent calculations of self-energy corrections due to hole-hole correlation effects.

I. INTRODUCTION

The optical properties of nickel and their relation to the electronic band structure have been the subject of many investigations.[1] It is only recently, however, that a clear picture has emerged of the band structure, and this is due largely to the acquisition of high-quality angle-resolved photoemission data using synchrotron radiation.[2,3] In this paper we describe a ferromagnetic band structure for Ni which has been obtained empirically by fitting the angle-resolved photoemission results. We show that it leads to predictions for the optical absorption and magneto-optical response which are in agreement with experiment. The exchange splitting in our empirical band structure is determined by requiring that we reproduce the experimental magneton number. The values thereby obtained for the exchange splitting and the Stoner gap are also in excellent agreement with angle-resolved and spin-polarized photoemission data. By adjustment of relatively few parameters, we have arrived at an empirical band structure which is capable of accounting for a large amount of data on Ni.

The organization of this paper is as follows. In the remainder of this Introduction we summarize the history of the photoemission properties of Ni, since the situation has evolved quite substantially over the last decade. Section II describes our empirical bands and the procedure used to obtain them. Section III describes the method of computation for the optical absorption and magneto-optical response. Numerical results for each of these two properties are presented and compared with experiment in Sec. IV. The previous work to which ours bears the closest resemblance is that of Wang and Callaway[4]; the difference is that they worked from first principles, whereas we have adopted a second-principles approach with empirical adjustments. The paper closes in Sec. V with some discussion on why the empirical bands differ from those obtained in first-principles calculations.

The very earliest photemission measurements on the valence bands of Ni indicated "anomalies." These anomalies might be summarized as follows: (1) the *exchange splitting*, expected on the basis of the band model of ferromagnetism, was found to be below the level of detectability[5] or rather small[6]; (2) the *width of the d bands* was found to be significantly smaller than that predicted by first-principles band calculations,[7] a result in distinct contrast with that for, say, Cu; (3) the *spin polarization* of photoelectrons failed to display the expected negative sign at threshold[8]; (4) a *satellite* was observed at about 6 eV below the Fermi level whose explanation must lie outside one-

electron band theory.[9] With the exception of (3), subsequent measurements have confirmed and refined these observations. In particular, angle-resolved photoemission measurements by Himpsel *et al.*[2] and by Eberhardt and Plummer[3] have determined the $E(\vec{k})$ relations, and have resolved the exchange splitting with some precision. Later measurements of the photoelectron spin polarization on better characterized samples have now shown the negative polarization at threshold,[10] but indicate small values for the Stoner gap (the separation between the top of the majority spin *d* band and the Fermi level) consistent with the small value of the exchange splitting. What we shall show is that these anomalies are linked with each other, and that they, and a large amount of other experimental data, can be accounted for by an empirical band structure in which two or three key parameters have been adjusted.

We shall not treat the 6-eV satellite. This is now known with some confidence to be a shake-up or excitonic[9,11] effect involving many-body correlations beyond the scope of the one-electron approach adopted here. It will be mentioned only incidentally in the theoretical discussion of Sec. V.

II. EMPIRICAL BAND STRUCTURE

We have used here the combined-interpolation-scheme approach described elsewhere,[12] and used in the earlier papers of this series.[13] The starting point was to fit the parameters of the scheme to a first-principles augmented-plane-wave (APW) calculation by Mattheiss.[14] To these bands we made *three* parameter adjustments. These adjustments, and the specific pieces of experimental data to which the parameters were fitted, are listed immediately below.

(1) d-band width. The width W of the *d* band was reduced by $\sim 25\%$ to achieve agreement with the angle-resolved photemission data of Refs. 2 and 3. In terms of the scheme this is done by scaling the Fletcher-Wohlfarth parameters, (A_{1-6} and Δ) as W and the hybridization coefficients (B_t and B_e) as $W^{1/2}$. (We are adopting here our previous nomenclature of the combined-interpolation scheme.[12])

(2) d-band position. The position of the *d* bands (parameter E_0) was adjusted upwards relative to the *sp* bands to obtain the correct distance of the *p*-like $L_{2'}$ level below the top of the *d* band. The angle-resolved photoemission measurements of Refs. 2 and 3 place $L_{2'}$ considerably lower than previously supposed. We regard this as perhaps the most important recent new piece of information on the band structure of Ni. As discussed earlier[15] and repeated below, this observation leads automatically to small values for the exchange splitting.

(3) Exchange splitting, Δ_{ex}. The relative positions of the majority- and minority-spin *d* bands were adjusted to reproduce the experimental magneton number (0.56 Bohr magnetons[16]). That is, the adjustments were performed in conjunction with precision calculations of the density of states, and it was required that the majority (minority) band contain exactly 5.28 (4.72) electrons per atom.

The band structure obtained is shown in Fig. 1 where it is compared with the experimental photoemission results of Refs. 2 and 3. It is seen that a quite reasonable overall fit can be obtained. Near the Fermi level, the experiments are able to resolve the exchange splitting. The quoted experimental values for Δ_{ex} (0.31 ± 0.03 eV from Ref. 2 and 0.26 ± 0.05 eV from Ref. 3) are in remarkably good agreement with our value of 0.310 eV obtained by the procedure described in (3) above. Strictly speaking one should consider the variation of Δ_{ex} with $\vec{k}$ and with orbital character,[3,17] but this has

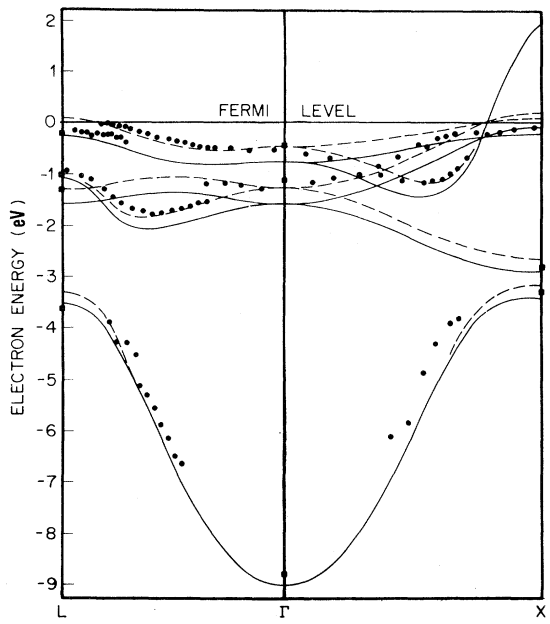

FIG. 1. Comparison of the empirically adjusted bands with the angle-resolved photoemission data of Ref. 2 (circles) and Ref. 3 (squares). The full (dashed) curves represent the majority (minority) spin bands.

not been done here; Δ_{ex} has been treated as a constant. The parameters of the combined interpolation scheme required to generate the bands of Fig. 1 are listed in Table I. Also listed are the parameters obtained by fitting the original APW calculation of Mattheiss.

The way in which the position of $L_{2'}$ influences the self-consistent value of Δ_{ex} is illustrated in Fig. 2. This figure shows the integrated density of states, expressed in electrons per atom, for the majority- and minority-spin band structures in the region of E_F. The discontinuities in slope mark the tops of the respective d bands. Since $L_{2'}$, and hence the entire sp complex, lies lower than in first-principle calculations, this has the effect of drawing a substantial fraction of an sp electron below E_F. Thus the energy which just encloses 5.28 electrons/atom in the majority-spin band structure lies just above the top of the d band. Specifically, we obtain a value of $\delta=0.100$ eV for the Stoner gap. Likewise, we are led to the rather small values $\Delta_{ex}=0.310$ eV for the exchange splitting. Had we not adjusted the position of $L_{2'}$ downwards, it would have been necessary to make a rather large excursion along the shallow slope portion of the curve to find 5.28 electrons. This necessity appears to be built in to all the attempts to calculate the band structure of ferromagnetic Ni from first principles.[4,18]

The anisotropy of the Stoner gap is relevant to spin-polarized photoemission experiments near threshold.[10,19] For normal emission from the (100) and (111) crystal faces, our values for the Stoner gap are $\delta_X=0.100$ eV and $\delta_L=0.263$ These correlate well with the experimental values for the frequency above threshold at which the spin polarization changes sign: 0.075 eV for (100) and 0.270 eV for (111). The crossover is expected to be comparable with the appropriate value of the Stoner gap.[19,20]

To summarize so far, what we have done is to vary three key parameters to achieve a reasonable match to the known magneton number and to the $E(\vec{k})$ relations derived from angle-resolved photoemission work. This has led automatically to values for Δ_{ex} in agreement with angle-resolved photoemssion and values for the Stoner gaps in agreement with spin-polarized photoemission. The

TABLE I. Parameters of the empirically adjusted band structure for ferromagnetic Ni compared with those obtained by fitting the first principles APW results for the paramagnetic Ni (energies in Ry). The Fermi energy in the empirical bands occurs at 0.67972 Ry.

	Empirical bands	First principles
E	0.646 09 (maj)	0.617 90
	0.668 88 (min)	
Δ	−0.001 97	−0.002 60
A_1	0.006 68	0.008 82
A_2	0.000 83	0.001 10
A_3	0.002 77	0.003 65
A_4	0.002 80	0.003 69
A_5	0.001 23	0.001 63
A_6	0.001 93	0.002 55
α	0.013 74	0.013 74
V_{000}	0.0611	0.0611
V_{111}	0.1158	0.1158
V_{200}	0.1186	0.1186
V_{220}	0.0540	0.0540
V_{311}	0.0822	0.0822
V_{222}	0.1140	0.1140
R	0.302	0.302
B_t	1.591	1.828
B_e	1.591	1.828
S	1.539	0.920
ξ	0.0067	0

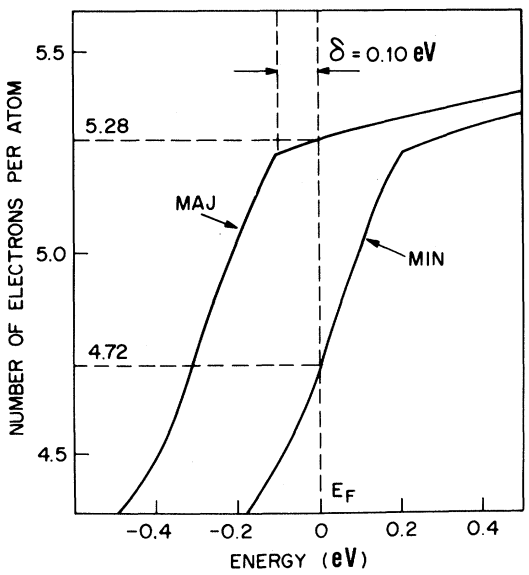

FIG. 2. Integrated density of states for the two spin bands in the vicinity of E_F.

additional consistency of the experimental $E(\vec{k})$ relations with Fermi surface data has already been noted.[2] In the next sections we investigate the extent to which our empirical band structure can account for the optical absorption and magneto-optical properties of Ni. It should be mentioned that need for major adjustments to the one-electron band structure is not universally accepted. Kleinman *et al.*[21] have argued, primarily on the basis of angle-resolved photoemission data from Smith *et al.*,[22] that the one-electron bands are adequate. The weight of evidence, however, is presently in favor of the adjustments. Specific to the concerns of this paper, the agreement for the optical absorption and magneto-optical response to be elaborated upon in Sec. IV would not be possible without the adjustments.

A further adjustment was made in our calculation; the orthogonalization parameter S was increased slightly. This has no effect on the preceding arguments, and was done to improve agreement with photoemission data for the positions of the lowest unoccupied levels of X_1 and L_1 symmetry. A comparison between the theoretical and experimental energy eigenvalues at high symmetry points is given in Table II.

TABLE II. Comparison between band energies for Ni determined from angle-resolved photoemission with those reproduced by the empirically adjusted band model. Energies are expressed in eV relative to the Fermi level. Levels denoted by angular brackets denote the unresolved mean for both spins.

	Experimental		This
	Ref. 2	Ref. 3	work
Occupied levels			
$\langle\Gamma_1\rangle$		−8.8	−9.04
$\langle\Gamma_{25'}\rangle$	−1.2	−1.1	−1.44
$\langle\Gamma_{12}\rangle$	−0.5	−0.4	−0.62
$\langle X_1\rangle$	−3.8	−3.3	−3.31
$\langle X_3\rangle$		−2.8	−2.78
$\langle X_2\rangle$		−0.85	+0.06
$X_{5\uparrow}$	−0.1		−0.10
$\langle L_1\rangle$	−3.4	−3.6	−3.43
$\langle L_3\rangle$		−1.3	−1.40
$\langle L_{2'}\rangle$	−0.9	−1.0	−1.04
$L_{3\uparrow}$	−0.15	−0.2	−0.26
$\langle W_{2'}\rangle$		−2.6	−2.70
$\langle W_3\rangle$		−1.7	−2.01
$\langle W_1\rangle$		−0.65	−0.75
$W_{1'\uparrow}$		−0.15	−0.10
$\langle K_1\rangle$		−3.1	−2.81
$\langle K_1\rangle$		−3.1	−2.52
$\langle K_3\rangle$		−0.9	−1.39
$\langle K_3\rangle$		−0.45	−0.57
Unoccupied levels			
$\langle X_1\rangle$	9.5	9.8	9.59
$\langle L_1\rangle$	6.0		5.87

III. COMPUTATION OF THE OPTICAL RESPONSE

The optical response of a ferromagnet is expressed in terms of the conductivity tensor σ. In the case of a cubic material with magnetization along the z axis, this takes the form[23]

$$\sigma=\begin{pmatrix}\sigma_{xx} & \sigma_{xy} & 0\\ -\sigma_{yx} & \sigma_{yy} & 0\\ 0 & 0 & \sigma_{zz}\end{pmatrix}. \tag{1}$$

The ordinary optical properties are determined by the diagonal components. The contribution of direct interband transitions to the real (i.e., absorptive) part of the conductivity is given by the Brillouin-zone integral[4,23]

$$\mathrm{Re}[\sigma_{xx}(\omega)]=\frac{e^2}{8\pi^2m^2\omega}\sum_{f,i}\int_{\mathrm{BZ}}d^3k\,|(\pi_{fi})_x|^2\delta(E_f-E_i-\hbar\omega)\,, \tag{2}$$

where $E_f(k)$ and $E_i(k)$ are the energies in final and initial bands f, i, respectively, and $(\pi_{fi})_\alpha$ is a Cartesian component ($\alpha=x,y,z$) of the matrix element of the operator $\vec{\pi}$, related to the usual momentum operator by the standard expression

$$\vec{\pi}=\vec{\mathbf{P}}+\left[\frac{\hbar}{4mc^2}\right]\vec{\sigma}\times\vec{\nabla}V(\vec{\mathbf{r}})\,. \tag{3}$$

For Bloch functions we may write[24]

$$\vec{\pi}=\frac{m}{\hbar}\frac{\partial H(\vec{k})}{\partial \vec{k}} . \tag{4}$$

In the presence of both an exchange splitting *and* spin-orbit interaction, the off-diagonal term σ_{xy} is nonzero. It can be determined experimentally through the measurements on the magneto-optical Kerr effect (MOKE).[25,26] The imaginary part of σ_{xy} is the absorptive part, and the interband contribution to it is given by[4,23]

$$\mathrm{Im}[\sigma_{xy}(\omega)]=\frac{e^2}{8\pi^2 m^2 \omega}\sum_{f,i}\int_{\mathrm{BZ}} d^3k\ \mathrm{Im}[(\pi_{fi})_x(\pi_{fi})_y]\delta(E_f-E_i-\hbar\omega) . \tag{5}$$

Equation (5) is very similar to Eq. (2); each is essentially the joint density of states with a weighting factor.

These expressions were evaluated numerically by the same methods used in previous papers of the series.[13] Calculations were performed both with and without inclusion of spin-orbit splitting. The spin-orbit parameter ξ was set equal to 0.0067 Ry, a value found by Wang and Callaway,[4] and which is slightly larger than the atomic value of 0.0055 Ry.

IV. RESULTS AND COMPARISON WITH EXPERIMENT

A. Overview: 0→30 eV

Theory and experiment for the optical absorption of Ni are compared over the photon energy range $\hbar\omega=0-30$ eV in Fig. 3. The experimental data are taken from Weaver *et al.*[27] We choose to plot here the quantity $(\hbar\omega)\epsilon_2$ which is equal to $4\pi\hbar\mathrm{Re}[\sigma_{xx}(\omega)]$. In this subsection, and those immediately following, we shall present results of calculations performed *without* spin-orbit coupling. The majority and minority band structures are then distinct from each other, and this facilitates the numbering of the bands and the display of the band-by-band decompositions, $\epsilon_2(i\rightarrow f)$, where i and f denote, respectively, the indices of the initial- and final-state bands. Introduction of spin-orbit effects is deferred to Secs. IV D and IV E.

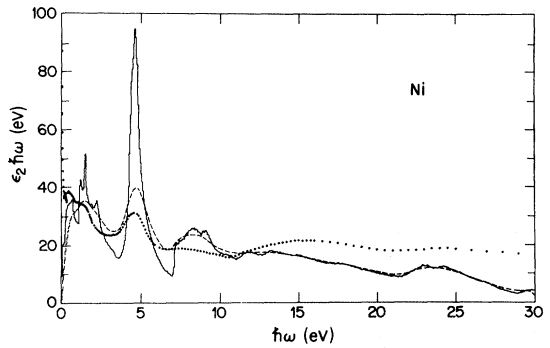

FIG. 3. Comparison between the calculated optical absorption (histogram) and experimental data (circles) from Ref. 27. The dashed curve is the calculated absorption after inclusion of lifetime broadening effects.

Over the 30-eV range of Fig. 3, it is seen that the agreement between theory and experiment is quite good for locations of the main maxima, minima, and broader structures. The theoretical structures are much sharper than those seen experimentally, the most dramatic example being the intense and narrow theoretical peak at $\hbar\omega\sim4.7$ eV. This suggests a strong need to include lifetime broadening effects. As an approximate way of doing this, we convolved each partial contribution $\epsilon_2(i\rightarrow f)$ with a Lorentzian broadening function of full width at half maximum (FWHM), $2\Gamma_i$. The values of Γ_i were taken from the experimental results in Fig. 7 of Ref. 3 at the mean energies of bands $i=1-5$. The effects on the theoretical ϵ_2 of this broadening are represented in the dashed curve in Fig. 3. It is seen that there are improvements in comparison with experiment. In particular, the intense peak at ~4.7 eV is considerably reduced and is now quite close in magnitude to the corresponding experimental peak. Since there is no arbitrary scaling factor in Eq. (2), the comparison for the absolute magnitude of ϵ_2 is significant.

B. Higher frequencies: $\hbar\omega\gtrsim7$ eV

At $\hbar\omega\sim7$ eV there is a pronounced minimum in the theoretical $(\hbar\omega)\epsilon_2$ curve followed by a sharp edge and a number of structures extending up to 30 eV. This behavior is very reminiscent of that noted earlier in Rh and Pd,[13] where the corresponding minima occur at 9.0 and 8.9 eV,

respectively. The edge in all these cases is attributed to the onset of transitions into band 7, specifically in the partial contribution $\epsilon_2(4\rightarrow 7)$. This is seen in Fig. 4 which shows the individual $\epsilon_2(i\rightarrow f)$ contributions for $f=7-10$ for both the majority- and minority-spin band structure. (Bands are numbered consecutively in increasing order of energy within each individual spin band structure). As expected in this energy range, the differences between the majority and minority contributions are small.

There is a broad peak in the theoretical ϵ_2 in the range $7-10$ eV having substructures: a shoulder at 7.3 eV, and peaks at 8.3 and 9.1 eV. A corresponding broad feature can be seen in the experimental data. It is much weaker, even after allowance for lifetime broadening, and the substructures are not resolved. It should be remembered that the "6-eV" many-body satellite can be excited in this energy range, and a simple lifetime broadening correction is probably inadequate to describe its effect on the ϵ_2 spectrum. Although the substructures are not observed in the experimental ϵ_2, they are readily resolved in modulated reflectance data. In Fig. 5 we reproduce the thermoreflectance measurements of Ni of Hanus *et al.*[28] Three structures are observed at 7.1, 8.3, and 9.5 eV. Hanus *et al.* do not comment on these structures in their original paper, and, as far as we are aware, there has been no subsequent attempt at identification. Referring back to Fig. 4 the identifications are straightforward. The onset at 7.0 eV is attributed

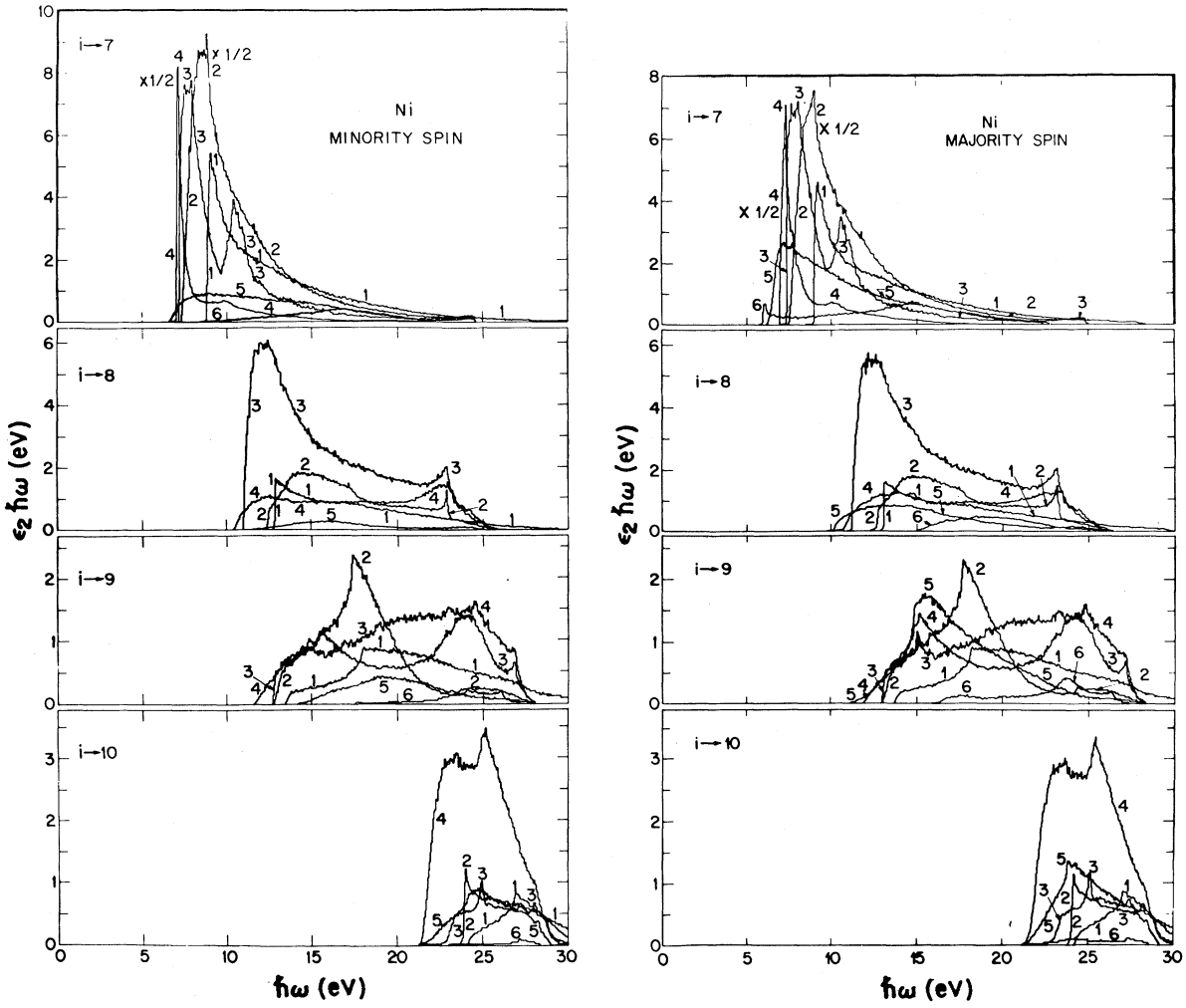

FIG. 4. Band-by-band decompositions, $\epsilon_2(i\rightarrow f)$, for the optical absorption of Ni involving transitions into bands $f=7-10$.

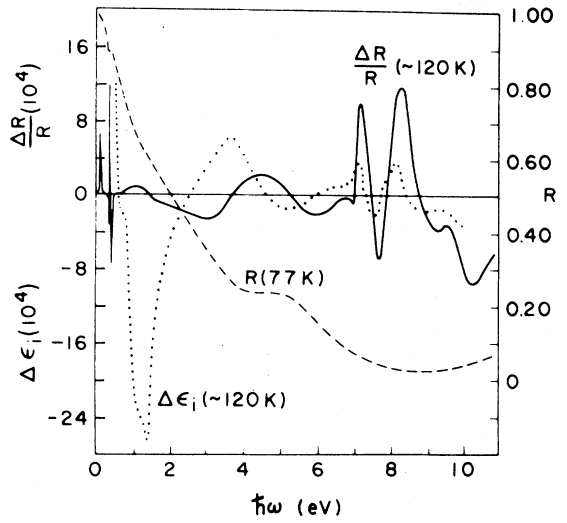

FIG. 5. Thermomodulation reflectance data on Ni by Hanus *et al.* (Ref. 27) showing the prominent structures in the 7—9 eV range.

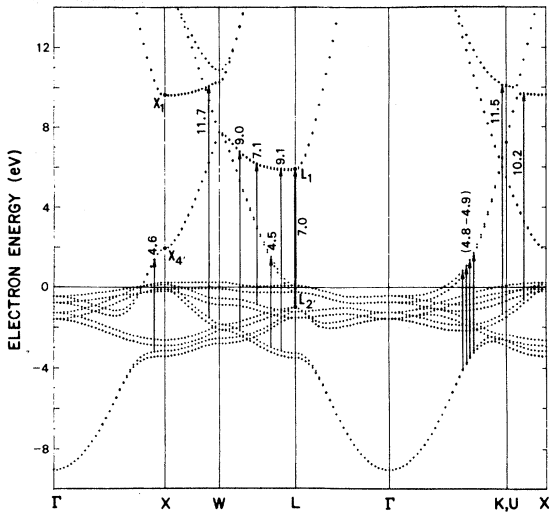

FIG. 6. Empirical band structure of Ni indicating the k-space locations of transitions responsible for prominent structures in the optical absorption in the range $\hbar\omega > 4$ eV.

the edge and peak in $\epsilon_2(4\rightarrow 7)$ for the minority bands; this is followed by very similar structure in the majority $\epsilon_2(4\rightarrow 7)$ but shifted upwards in energy by about 0.2 eV. The peak at 8.3 eV is a composite structure arising through peaks in $\epsilon_2(2\rightarrow 7)$ at around this energy in both spin band structures; a smaller peak in $\epsilon_2(3\rightarrow 7)$ also makes a contribution to this feature. The peak at 9.5 eV is attributable to the sharp onset in $\epsilon_2(1\rightarrow 7)$ for both spin band structures; this feature has some composite character since $\epsilon_2(2\rightarrow 7)$ for the majority-spin bands also has a peak near this energy. Assignments for the k-space locations of the ~ 7.1 eV and the ~ 9.3 eV features are shown in Fig. 6. The transitions shown are on the $Q(WL)$ symmetry line. The appropriate band pairs are seen to be quite parallel, thus accounting for a high joint density of rates.

Between the minima at 11 and 21.5 eV in the theoretical $(\hbar\omega)\epsilon_2$ there is a broad structure. This is seen in the experimental data. It is identified as a composite structure due to transitions into bands 8 and 9. The theoretical peaks at about 23—24 eV also have a weak counterpart in the experimental data. There are also composite structures involving transitions into bands 8 and 9. Transitions into band 10 also contribute, with $\epsilon_2(4\rightarrow 10)$ being particularly strong.

In the region above 11 eV, the experimental absorption is consistently higher than theory. This discrepancy has been noted previously[13] and may represent an experimental problem rather than a fundamental disagreement. At these short wavelengths, surface scattering becomes increasingly important, and so a specular reflectance measurement will tend to overestimate the absorptance. There are also uncertainties due to the high-frequency extrapolation in the Kramers-Krönig inversion of the data.

C. The 4.7-eV peak

The most intense feature in the theoretical $(\hbar\omega)\epsilon_2$ spectrum is the sharp peak at about 4.7 eV. This agrees in energy with a well-established experimental peak. After inclusion of lifetime broadening effects, the agreement between theory and experiment for the magnitude (as well as position) of the peak is quite good. Reference to Fig. 7 shows that the peak originates in $\epsilon_2(1\rightarrow 6)$. The locations of the transitions in k space are indicated in Fig. 6. The transitions occur primarily along the Σ direction, where bands 1 and 6 are seen to be quite parallel over an extended region. Contributions to this $\epsilon_2(1\rightarrow 6)$ peak are also permitted from transitions near X and L.

Our assignment above is the same as that made by Wang and Callaway.[4] In their work, however, the peak is predicted to occur at about 1 eV higher in photon energy. The improvement in agreement in our work is directly attributable to the empirical adjustments we have made to the first-principles band structure, particularly the narrowing of the d bands. The good agreement which we obtain for this peak therefore provides strong support for the

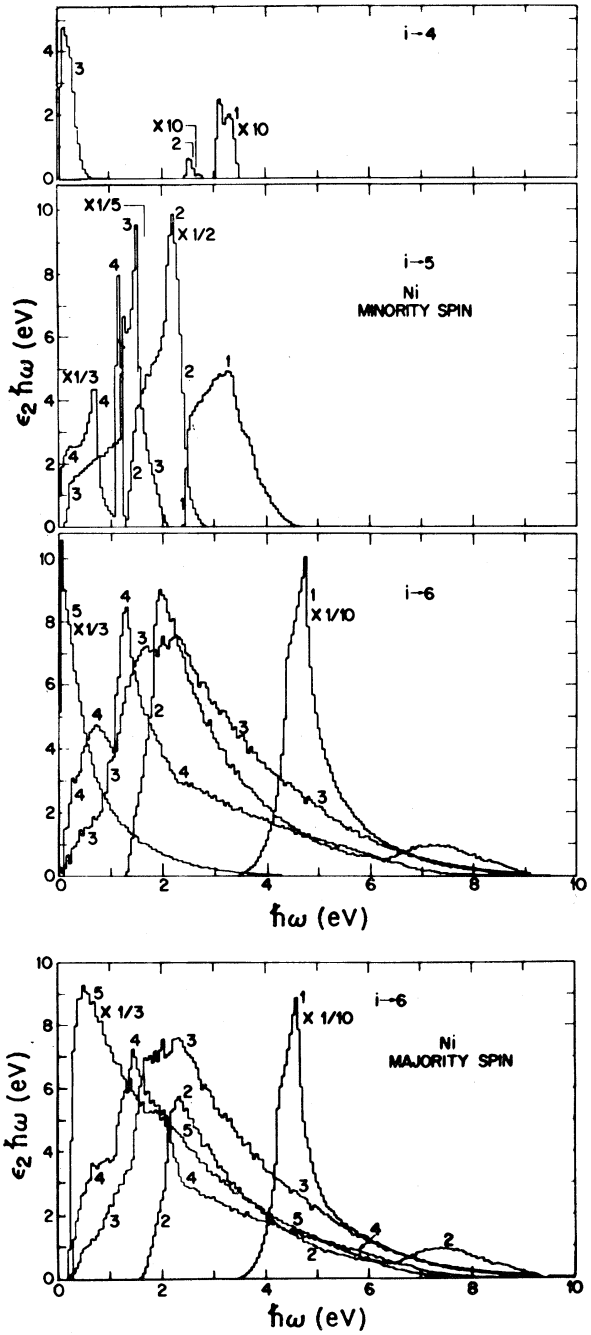

FIG. 7. Band-by-band decompositions, $\epsilon_2(i \rightarrow f)$, for the optical absorption of Ni involving transitions into bands $f=4,5,6$.

modifications to the band structure as determined by the angle-resolved photemission data.[2,3]

D. Low frequencies: $\hbar\omega \lesssim 3$ eV

At the lower photon energies, effects due to exchange splitting are predicted to be more conspicuous. In Fig. 7 it can be seen that in the majority-spin band structure $\epsilon_2(5 \rightarrow 6)$ vanishes below about 0.2 eV, whereas the corresponding contribution for the minority-spin band structure continues all the way down to zero frequency. Also, there are significant contributions $\epsilon_2(i \rightarrow 4)$ and $\epsilon_2(i \rightarrow 5)$ for the minority bands, because bands 4 and 5 are partially unoccupied. This should therefore be the frequency region in which magnetic effects are most observable. In particular, we would expect significant changes on passing through the Curie temperature T_C.

Experiment and theory are compared for this low-frequency region in Fig. 8. The dotted histogram in Fig. 8 is the theoretical $(\hbar\omega)\epsilon_2$ computed with inclusion of spin-orbit splitting. This brings about a dramatic change at the extreme low frequencies with the introduction of a strong peak in the 0.1-eV region. There are changes also in the form of the multiple structure in the $\hbar\omega \sim 1.1-1.6$ eV range. Elsewhere the effects of spin-orbit splitting are rather small. Let us now discuss in turn the three principal structure groupings in this low-energy region.

1. 0.2—0.7 eV

The experimental data of Fig. 8 show a peak at 0.28 eV. This is followed by a minimum at 0.4 eV and a broad peak in the 0.5—0.7 region. We identify these structures with the structures in the same energy range in the dotted histogram of Fig. 8. These transitions occur in the k-space localities indicated as a and a' in Fig. 9. In the absence of spin-orbit coupling, transitions a occur in the minority-spin band structure between bands 4 and 5; the transitions a' occur between bands 5 and 6 in the majority-spin band structure.

2. 1.1—1.6 eV

In the range $\hbar\omega = 1.1-1.6$ eV, our calculations shown in Fig. 8 predict a prominent set of structures. These are modified quite appreciably by the inclusion of spin-orbit splitting. These structures are attributed to transitions in the $\vec{k}$-space vicinity of those labeled b and b' in Fig. 9. The corresponding experimental structure is seen only weakly in Fig. 9, but has been widely documented.[1,28] We display in Fig. 10 the data of Stoll[29] which brings out somewhat better the structure in the 1.1—1.6 eV range.

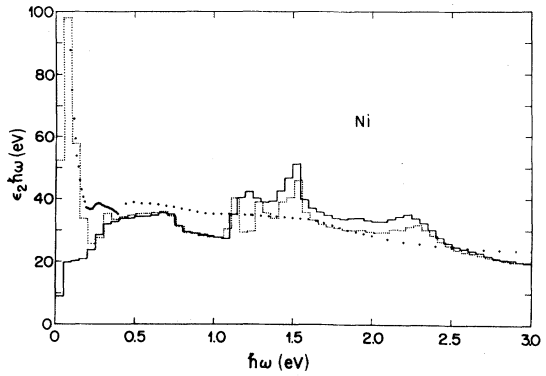

FIG. 8. Calculated optical absorption of Ni both with (dotted histogram) and without (full histogram) inclusion of spin-orbit splitting. The full circles are the experimental data from Ref. 27.

The transitions designated b in Fig. 9 occur within the minority-spin band structure. The final states are only just above E_F. On passing through T_C into the paramagnetic state, the final-state band for these transitions will fall below E_F and thereby become occupied. The b transitions are therefore expected to disappear on passing through T_C. The transitions b', on the other hand, occur between bands 5→6 for both spins, and should therefore survive passage through T_C. The data of Stoll in Fig. 10 shows some evidence for these expectations. At the lowest temperature (77 K) there is a broad structure in the σ/c with two substructures at about 1.0 and 1.5 eV. At the highest temperature (500 K) there is a single peak at about 1.2 eV. We interpret this as the disappearance of the b transitions and the consolidation of the b' transitions at the common energy.

3. *The 2.3-eV structure*

The theoretical calculations of Fig. 8 show a peak at $\hbar\omega \sim 2.3$ eV. From the $\epsilon_2(i \rightarrow f)$ decompositions of Fig. 7, we identify this structure with transitions between bands 2→5. The $\vec{k}$-space locations are labeled as c in Fig. 9. Since these transitions occur entirely within the minority-spin band structure with final states just abour E_F, there should be a substantial change on passing through T_C.

The data of Stoll[29] (Fig. 10) do show a weak set of structures at about 2.3 eV, and there is an appreciable temperature dependence. It should be mentioned, however, that these structures are not well established. Some workers report a profusion

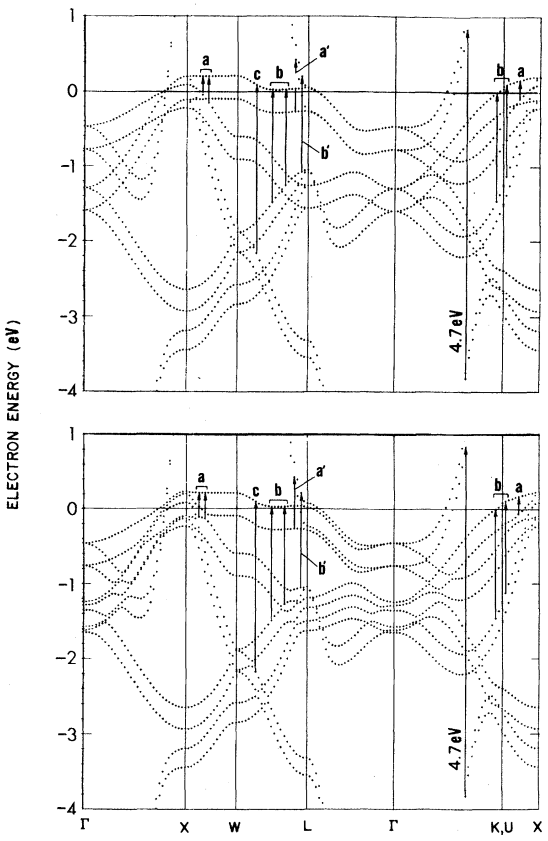

FIG. 9. Band structure of Ni in the d-band range calculated both with (lower part) and without (upper part) the inclusion of spin-orbit splitting. The arrows indicate k-space locations of transitions responsible for observed absorption structures.

of structures in this range.[30] Others find none.[31] Studna,[32] using high-resolution ellipsometric techniques, has detected a single very weak structure at 2.36 eV. On balance, therefore, there does seem to be experimental evidence for a 2.3-eV structure, but it is much weaker than that predicted theoretically. Note that the transition c with which we have identified this structure is between initial and final states which are both predominantly d-like. Since $d \rightarrow d$ transitions are forbidden in the purely atomic case, the predicted magnitude of this structure is presumably very sensitive to the details of the *sp-d* hybridization in our parametrization scheme.

Note that the transitions c occur from states in the lower d-band region to the uppermost d band, thus providing an estimate of the d-band width. The agreement between our model and the experi-

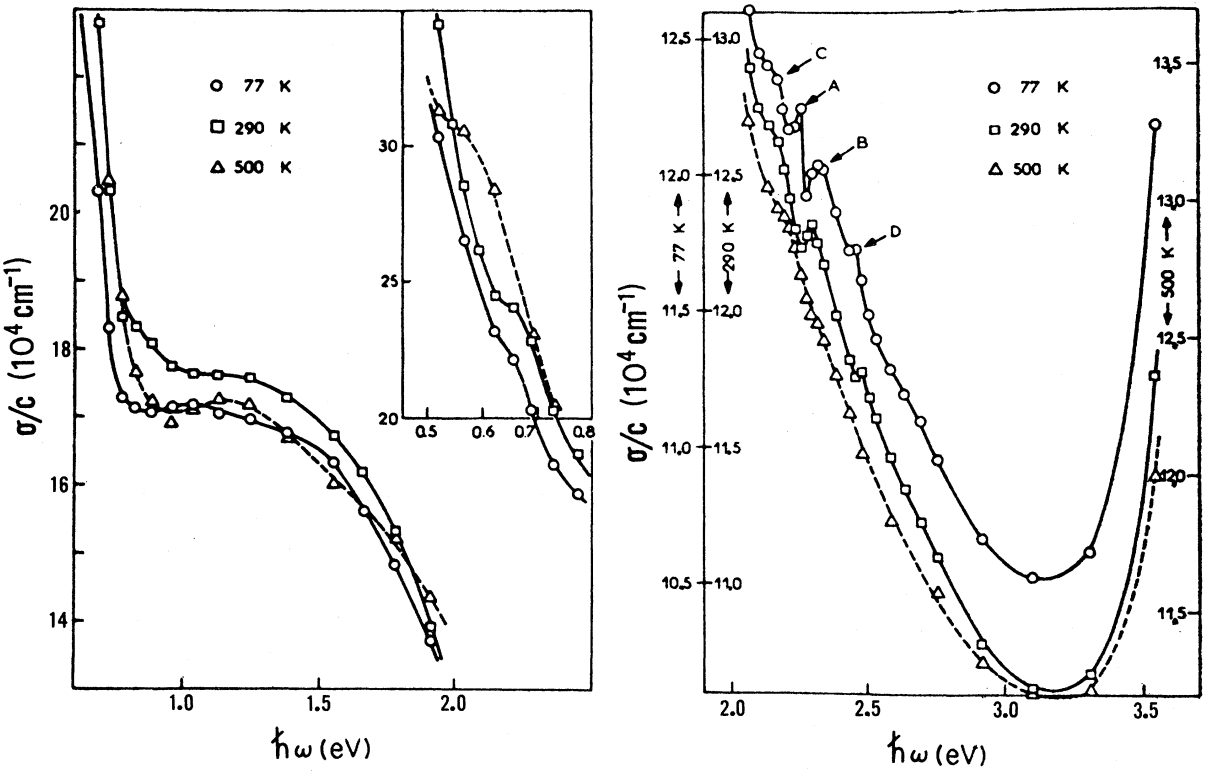

FIG. 10. Experimental optical absorption data on Ni by Stoll (Ref. 29) showing the well-established structure around $\hbar\omega \sim 1.4$ eV and the less well-established features close to $\hbar\omega \sim 2.3$ eV.

mental data for the energy of this feature provides further support for the narrowing of the d bands.

E. Magneto-Optical Response

Our calculations for the dissipative part of the off-diagonal conductivity σ_{xy} are shown in Fig. 11, where they are compared with the experimental values obtained from MOKE data.[25,26] The comparison is much less satisfying than for the diagonal conductivity, but there are nevertheless some significant features of agreement.

At the lowest frequencies ($\hbar\omega \lesssim 0.5$ eV) σ_{xy} is negative in both theory and experiment. This is attributable to the predominance of contributions from the minority-spin band structure, very analogous to the situation in spin-polarized photoemission at threshold.[10,20] The experimental σ_{xy} switches sign at $\hbar\omega \sim 0.4$ eV. The theoretical σ_{xy}, however, remains negative over this range. The experimental σ_{xy} has a maximum at 3.2 eV followed by a minimum at 4.6 eV. We identify these features with corresponding behavior in the theoretical σ_{xy}, where a maximum at 4.2 eV is followed by a minimum at 4.7 eV.

The failure of the theoretical model to reproduce the correct sign for σ_{xy} is not too surprising. The weighting factor $\mathrm{Im}[(\pi_{fi})_x(\pi_{fi})_y]$ in the integrand of Eq. (5) can occur with either sign. In summing over the various band pairs f, i, there are a number of comparable contributions of alternating sign, so that the magnitude and sign of the final result is sensitive to details of the parametrization.

The locations of structures may still be of significance, however, and we identify the experimental peak at 1.4 eV with the theoretical maximum at the same energy. The optical transitions involved here are also responsible for structure in the same energy region in ϵ_2, and their k-space locations are designated as b and b' in Fig. 9.

The very dramatic behavior of the theoretical σ_{xy} in the 4–5 eV range can also be located in $\vec{k}$ space. It is associated with the transitions between bands $1 \rightarrow 6$ located along the ΓK direction and indicated in Fig. 6. As discussed in Sec. IV C, these give rise to a very prominent peak in ϵ_2. Referring to Fig. 7, it can be seen that this feature in $\epsilon_2(1 \rightarrow 6)$ is essentially the same in both spin and band structures but is displaced slightly to higher

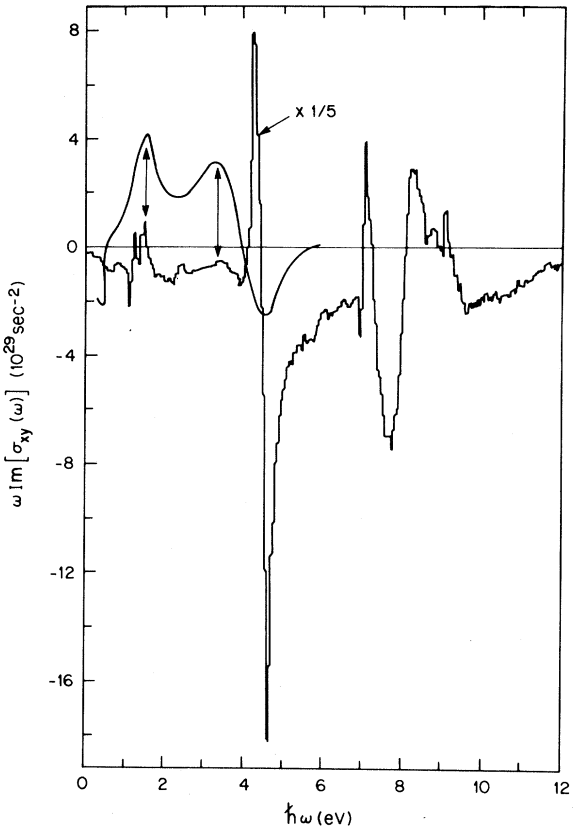

FIG. 11. Calculated results (histogram) for the dissipative part of the off-diagonal conductivity, $\mathrm{Im}\sigma_{xy}$, compared with the experimental results of Ref. 26 (smooth curve).

photon energies for the minority spins. On the low-energy, rapidly rising portion of this peak, contributions from the majority-spin band structure predominate, leading to a positive sign for σ_{xy}. Conversely, minority-spin contributions predominate on the falling side of the peak, leading to a negative σ_{xy}. The MOKE response for this feature is therefore expected to resemble the derivative of the optical absorption. This particular ordering might seem surprising. Because of the exchange splitting, the minority d bands lie higher in energy than the majority d bands, so that transitions from d-band initial states at any point in k space should occur at *lower* photon energies for minority spins. The reason for the reversal of this expectation is that the transitions involved here occur across the *sp-d* hybridization gap. The initial and final states both have some d character, and in this instance the exchange splitting is greater for the *final*-state bands. Consequently, the minority-spin contribution is shifted to *higher* photon energies relative to the majority-spin contribution, bringing about the positive- to negative-sign sequence in agreement with experiment.

The 4—5 eV feature is much sharper in theory than in the experimental MOKE data. This points once again to the desirability of including lifetime broadening, as pointed out previously by Wang and Callaway.[4] Since the initial states are well removed from E_F, the broadening should be quite large.[3] The calculations of σ_{xy} by Wang and Callaway predict a similar strong structure, but place it about 1 eV higher in photon energy. The lower energy and therefore closer agreement with experiment in our calculations is once again directly attributable to our empirical adjustments to the first-principles results. Note that the energy position of the positive-to-negative feature in σ_{xy} cannot be simply equated to the d-band width, as attempted previously.[26] Indeed, the agreement obtained in the present work provides further support for a significantly narrowed d band as suggested by photoemission data.

V. THEORETICAL DISCUSSION

What we have demonstrated above is that if one makes adjustments to only the width and position of the d bands of Ni to agree with angle-resolved photoemission data and the experimental magneton

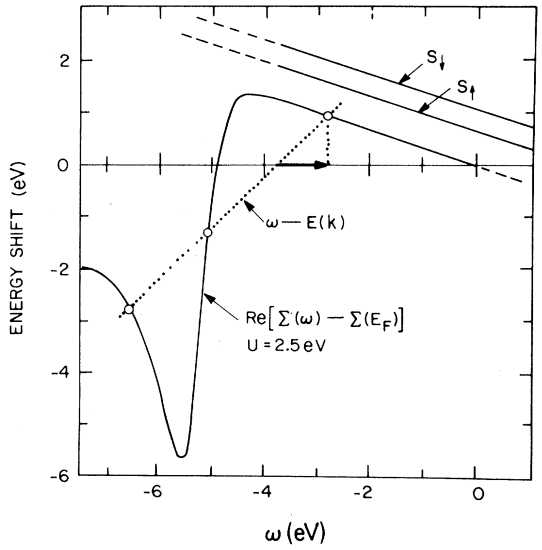

FIG. 12. The empirical adjustments to the one-electron band structure, represented here as the energy-dependent shifts $S_\uparrow$ and $S_\downarrow$, are compared with the theoretical results of Ref. 34 for $\mathrm{Re}\Sigma$, the real part of the self-energy correction due to hole-hole correlation effects.

number, a gratifyingly large amount of additional data immediately falls into place: namely, the exchange splitting, the Stoner gap and its anisotropy, the Fermi surface, the optical absorption, and the magneto-optical response. The empirical band structure arrived at differs significantly from those obtained by conventional one-electron band calculations using realistic potentials. In this section we discuss briefly the reasons which have been proposed for this difference.

Within the framework of one-electron band theory, our two key adjustments (i.e., an *increase* of the mean energy of the d band, coupled with a *decrease* of the d-band width) are inconsistent with each other. As one raises the energy position of the d resonance, its lifetime against tunneling through the $l=2$ centrifugal potential decreases, leading to an *increased* d-band width. This expectation is amply borne out by numerical band calculations using a variety of one-electron potentials.[18]

Current theoretical explanations[33,34] of the photoemission anomalies in Ni consider the corrections to the self-energy $\Sigma_{n\sigma}(\omega,\vec{k})$ due to intra-atomic correlations between the $3d$ electrons. The spectral function of the created hole state is written

$$A_{n\sigma}(\omega,\vec{k})=\frac{1}{\pi}\frac{\mathrm{Im}\Sigma_{n\sigma}(\omega,\vec{k})}{[\omega-E_{n\sigma}(\vec{k})-\mathrm{Re}\Sigma_{n\sigma}(\omega,\vec{k})]^2+[\mathrm{Im}\Sigma_{n\sigma}(\omega,\vec{k})]^2}\ , \tag{6}$$

where $E_{n\sigma}(\vec{k})$ are the one-electron band energies. Such theories can account qualitatively for both the existence of the satellite structure and the narrowing of the d band. The latter arises through the differential energy shifts across the d band represented by the real part of the self-energy $\mathrm{Re}\Sigma_{n\sigma}(\omega,\vec{k})$. Initially, the theories encountered quantitative difficulties in accounting simultaneously for the magnitudes of the satellite binding energy and the d-band narrowing. Liebsch[34] has argued recently that this problem is removed by proceeding beyond the low-density approximation.

The empirical adjustments we have made to width and position of the d-band may be represented equivalently as shifts $S_\uparrow$ and $S_\downarrow$ which are linear in energy. These are shown in Fig. 12 where they are compared with the corresponding values of $\mathrm{Re}[\Sigma(\omega)-\Sigma(E_F)]$ obtained numerically by Liebsch.[34] Over the energy range of the d band, $\Sigma(\omega)$ varies in a very linear fashion, and the slope (directly related to the d-band narrowing) is equal to the slopes of the experimental lines $S_\uparrow$ and $S_\downarrow$. This is not unexpected since Liebsch chose the magnitude of the intra-atomic hole-hole Coulomb interaction ($U=2.5$ eV) to reproduce the measured d-band width. The achievement in the results for $\Sigma(\omega)$ in Fig. 12 is that they lead simultaneously to a spectral function having the two-hole-bound-state satellite at the same binding energy as that observed experimentally.

Note that the theoretical results for $\mathrm{Re}\Sigma(\omega)$ are averaged over band index, and spin, and are given only relative to the value at the Fermi level $\mathrm{Re}\Sigma(E_F)$. Our empirical curves $S_\uparrow$ and $S_\downarrow$, on the other hand are presented for the individual spins and on an absolute scale. The reason we are able to do this is that in our adjustment procedure we have treated the *sp* manifold as a stationary background over which the d manifold has been slid. The key piece of experimental information which fixes the d bands relative to the *sp* background is the distance of the top of the majority d band over the p-like level of $L_{2'}$ symmetry. This distance is given directly by the angle-resolved photoemission data,[2,3] and is significantly larger than predicted in the best and most recent one-electron band calculations. As stated in Sec. II, we regard this measurement as perhaps the most important new piece of information on the band structure of Ni.

Note added in proof. Professor J. L. Erskine has kindly drawn our attention to a paper by him [Physica 89B, 83 (1977)], which presents MOKE data up to the photon energy 12 eV. A structure is seen at ~ 7 eV which, after suitable allowance for lifetime broadening, corresponds reasonably well to the structure in this range in the theoretical results of Fig. 11.

ACKNOWLEDGMENT

We thank J. H. Weaver and F. J. Himpsel for communicating data in numerical form.

*Present address: Institüt für Festkörperforschung, KFA, D-517 Julich, Germany.
†Present address: Department of Physics, University of California, Berkeley, California.

[1]P. O. Nilsson, in *Solid State Physics,* edited by H. Ehrenreich, F. Seitz, and D. Turnbull (Academic, New York, 1974), Vol. 29, p. 139, and references therein.
[2]F. J. Himpsel, J. A. Knapp, and D. E. Eastman, Phys. Rev. B 19, 2919 (1979).
[3]W. Eberhardt and E. W. Plummer, Phys. Rev. B 21, 3245 (1980).
[4]C. S. Wang and J. Callaway, Phys. Rev. B 9, 4897 (1974).
[5]D. T. Pierce and W. E. Spicer, Phys. Rev. Lett. 25, 581 (1970).
[6]J. E. Rowe and J. C. Tracy, Phys. Rev. Lett. 27, 799 (1970).
[7]S. Hüfner, G. K. Wertheim, N. V. Smith, and M. M. Traum, Solid State Commun. 11, 323 (1972).
[8]U. Bänninger, G. Busch, M. Campagna, and H. C. Siegmann, Phys. Rev. Lett. 25, 383 (1970).
[9]S. Hüfner and G. K. Wertheim, Phys. Lett. 47A, 349 (1974); 51A, 299 (1976); P. C. Kemeny and N. J. Shevchik, Solid State Commun. 17, 255 (1975); C. Guillot, Y. Ballu, Y. Paigné, J. Lecante, K. P. Jain, P. Thiry, R. Pinchaux, Y. Petroff, and L. Faljcov, Phys. Rev. Lett. 39, 1632 (1977); M. Iwan, F. J. Himpsel, and D. E. Eastman, *ibid.* 43, 1829 (1979).
[10]W. Eib and S. F. Alvarado, Phys. Rev. Lett. 37, 444 (1976).
[11]D. R. Penn, Phys. Rev. Lett. 42, 921 (1979); L. C. Davis and L. A. Feldkamp, *ibid.* 44, 673 (1980).
[12]N. V. Smith, Phys. Rev. B 19, 5019 (1979).
[13]R. Lässer, N. V. Smith, and R. L. Benbow, Phys. Rev. B 24, 1895 (1981); R. Lässer, and N. V. Smith, *ibid.* 24, 1910 (1981).
[14]L. F. Mattheiss, private communication.
[15]N. V. Smith and S. Chiang, Phys. Rev. B 19, 5013 (1979).
[16]H. Danan, H. Herr, and A. J. P. Meyer, J. Appl. Phys. 39, 669 (1968).
[17]E. Dietz, U. Gerhardt, and C. J. Maetz, Phys. Rev. Lett. 40, 892 (1978); P. Heiman, F. J. Himpsel, and D. E. Eastman, Solid State Commun. 39, 219 (1981).
[18]J. W. D. Connolly, Phys. Rev. 159, 415 (1967); C. S. Wang and J. Callaway, Phys. Rev. B 15, 298 (1977).
[19]E. Kisker, W. Gudat, M. Campagna, E. Kuhlmann, H. Hopster, and I. D. Moore, Phys. Rev. Lett. 43, 966 (1979).
[20]E. P. Wohlfarth, Phys. Lett. 36A, 131 (1971); I. D. Moore and J. B. Pendry, J. Phys. C 11, 4615 (1978).
[21]L. Kleinman, W. R. Grise, and K. Mednick, Phys. Rev. B 22, 1105 (1980); L. Kleinman, *ibid.* 22, 6468 (1980).
[22]R. J. Smith, J. Anderson, J. Hermanson, and G. J. Lapeyre, Solid State Commun. 21, 459 (1977).
[23]J. L. Erskine and E. A. Stern, Phys. Rev. B 8, 1239 (1973).
[24]E. I. Blount, in *Solid State Physics,* edited by F. Seitz and D. Turnbull (Academic, New York, 1962), Vol. 13 p. 305.
[25]G. S. Krinchik and A. V. Artemiev, Zh. Eksp. Teor. Fiz. 53, 1901 (1967) [Sov. Phys.—JETP 26, 1080 (1968)].
[26]J. L. Erskine and E. A. Stern, Phys. Rev. Lett. 30, 1329 (1973).
[27]J. H. Weaver, C. Krafka, D. W. Lynch, and E. E. Koch, Appl. Opt. 20, 1124 (1981). This paper announces a forthcoming publication containing a larger compilation of optical data on the 3*d*, 4*d*, and 5*d* metals as well as tabulating a recommended set of optical constants for each metal.
[28]J. Hanus, J. Feinlieb, and W. J. Scouler, Phys. Rev. Lett. 19, 16 (1967); the derived $\Delta\epsilon_i$ of Fig. 5 (equivalent to $\Delta\epsilon_2$ in our nomenclature) was added by M. Cardona, in *Solid State Physics,* edited by F. Seitz, D. Turnbull, and H. Ehrenreich (Academic, New York, 1969), Suppl. 11, p. 133.
[29]M-P. Stoll, Solid State Commun. 8, 1207 (1970).
[30]M. M. Kirillova, Zh. Eksp. Teor. Fiz. 61, 336 (1971) [Sov. Phys.—JETP 34, 178 (1972)]; I. I. Sasovskaya and M. M. Noskov, Fiz. Met. Metallov. 32, 723 (1971); 33, 86 (1972).
[31]D. W. Lynch, R. Rosei, and J. H. Weaver, Solid State Commun. 9, 2195 (1971); B. W. Veal and A. P. Paulikas, Int. J. Magn. 4, 57 (1973).
[32]A. A. Studna, Solid State Commun. 16, 1063 (1975).
[33]L. C. Davis and L. A. Feldkamp, Solid State Commun. 34, 141 (1980); G. Treglia, F. Ducastelle, and D. Spanjaard, Phys. Rev. B 21, 3729 (1980); A. Liebsch, Phys. Rev. Lett. 43, 1431 (1979).
[34]A. Leibsch, Phys. Rev. B 23, 5203 (1981).